

DOE/BC/14882--9

Quarterly Technical
Progress Report
for

**Responsive Copolymers for Enhanced
Petroleum Recovery**

DE-AC22-92BC 14882

by

Charles McCormick
Roger Hester

Department of Polymer Science
University of Southern Mississippi
Hattiesburg, MS 39406

DISCLAIMER

This report was prepared as an account of work sponsored by an agency of the United States Government. Neither the United States Government nor any agency thereof, nor any of their employees, makes any warranty, express or implied, or assumes any legal liability or responsibility for the accuracy, completeness, or usefulness of any information, apparatus, product, or process disclosed, or represents that its use would not infringe privately owned rights. Reference herein to any specific commercial product, process, or service by trade name, trademark, manufacturer, or otherwise does not necessarily constitute or imply its endorsement, recommendation, or favoring by the United States Government or any agency thereof. The views and opinions of authors expressed herein do not necessarily state or reflect those of the United States Government or any agency thereof.

Contract Beginning Date September 22, 1992
Contract Second Year End Date September 21, 1994

Current Year DOE Award \$273,400

DOE/BC/14882--9
CC: 6/11/93
REVIEWED
DOE/BC/14882--9

Contracting Officer's Representative Jerry F. Casteel

for the time period of
June 23, 1994 through September 21, 1994

MASTER

DISTRIBUTION OF THIS DOCUMENT IS UNLIMITED

ma

DISCLAIMER

This report was prepared as an account of work sponsored by an agency of the United States Government. Neither the United States Government nor any agency Thereof, nor any of their employees, makes any warranty, express or implied, or assumes any legal liability or responsibility for the accuracy, completeness, or usefulness of any information, apparatus, product, or process disclosed, or represents that its use would not infringe privately owned rights. Reference herein to any specific commercial product, process, or service by trade name, trademark, manufacturer, or otherwise does not necessarily constitute or imply its endorsement, recommendation, or favoring by the United States Government or any agency thereof. The views and opinions of authors expressed herein do not necessarily state or reflect those of the United States Government or any agency thereof.

DISCLAIMER

Portions of this document may be illegible in electronic image products. Images are produced from the best available original document.

Summary of Technical Progress

A. Task I - Advanced Copolymer Synthesis

The primary objective is the synthesis of copolymers of maleic anhydride and ethyl vinyl ether followed by reaction with controlled amounts of octyl and dodecyl amines. A small concentration (ca. 1 mole%) of naphthalene labels with long spacer groups is also incorporated. Hydrolysis of the remaining anhydride groups yield water-soluble terpolymers with degrees of amidation ranging from 8 to 50 mole%. Key features of this study include variation in hydrophobe length and content, maintenance of a small quantity of naphthyl groups to avoid perturbation of the parent copolymers, and presence of comparatively large hydrophobes relative to naphthyl label. These terpolymers provide useful models for elucidating the nature of hydrophobic associations in systems having a random distribution of the hydrophobic groups.

Monomer and Polymer Synthesis

1-(7-Aminoheptyloxymethyl) naphthalene is prepared as follows (Scheme 1). Williamson etherification of 1-Chloromethylnaphthalene with the monosodium salt of 1,6-hexanediol affords 6-(1-naphthyl) methoxy-1-hexanol (**1**). Addition of sodium hydride to bulk 1,6-hexanediol to generate the respective sodium salt assures monosubstitution. Sulfonation is achieved by reaction of **1** with methanesulfonyl chloride in the presence of triethylamine as acid scavenger.¹ The sulfonate group is readily displaced by nucleophilic substitution with sodium cyanide in DMSO at elevated temperature to give **2**. To obtain the primary amine (**3**), the nitrile is reduced with lithium aluminum hydride.

Poly (maleic anhydride-*alt*-ethyl vinyl ether) (Scheme 3) is prepared by the addition of a slight excess of ethyl vinyl ether to a solution of 1.1 M maleic anhydride and 1.8 mM benzoyl peroxide in benzene under nitrogen at 60 °C. After 8 hours, the white precipitate (polymer **4**) that formed was filtered and dried under vacuum.

The parent polymer (**4**) is substituted with alkyl and naphthyl groups by addition of the modifying primary amine to a solution of **4** in ethyl acetate at room temperature under nitrogen (Scheme 3). The reaction is then allowed to proceed for 8 hours at 60 °C. Modified polymer **5** is isolated by precipitation of the reaction mixture into diethyl ether.

Hydrolyses of parent polymer anhydride groups are carried out in 1 N NaOH at room temperature. After complete dissolution, the solutions are dialyzed for one week (Spectra-Por[®] dialysis tubing, 12,000-14,000 molecular weight cutoff) and freeze-dried to give water-soluble polymer **6**.

Task 2. Characterization of Molecular Structure

¹H and ¹³C NMR spectra were recorded using a Bruker AC-200. A Mattson 2020 Galaxy Series FTIR was used to obtain infrared spectra. GC analysis was performed on a Hewlett Packard 5890 Series II Gas Chromatograph equipped with an Alltech Capillary Column AT-5. A Hewlett

Packard Model 1050 HPLC was used to determine the purity of solid samples. A waters Bondapak C₁₈ column was employed with methanol as the mobile phase. The sample effluent was typically monitored at 280 nm.

Terpolymer Solution Preparation

The appropriate amount of dried terpolymer **6** was weighed and then dissolved in water in a volumetric flask from which further dilutions of this stock solution could be made. The solutions were allowed to stand for two weeks prior to viscosity measurement. The pH value of each solution was obtained with a Corning 130 pH meter at room temperature.

UV Analysis

Ultraviolet spectroscopy was used in determining the naphthalene content in the terpolymers. All spectra were recorded with a Hewlett Packard 8452A Diode Array Spectrophotometer. Beer-Lambert plots were obtained for a naphthyl model compound (**4**)² and compared with polymer absorption.

Fluorescence Analysis

The concentrations of terpolymer solutions were 0.05 g/dL. The concentration of naphthyl moieties in these solutions varied from 2.5×10^{-6} to 3.0×10^{-6} M. Sample solutions were degassed by gently bubbling with helium. All the samples were excited at 280 nm, and monomer intensities were measured at 330 nm. Emission spectra of the terpolymers were recorded with a Spex Fluorolog-2 fluorescence spectrometer. Fluorescence decays were measured with a Photochemical Research Associates (PRA) single-photon-counting instrument equipped with a H₂-filled 510-B flashlamp. A nonlinear iterative deconvolution technique was used to fit the decay curves.

Low Angle Laser Light Scattering

Classical light scattering studies were performed with a Chromatix KMX-6 low-angle laser light scattering spectrophotometer with a 2-mW He-Ne laser operating at 633 nm. Refractive index increments (dn/dc) were obtained using a Chromatix KMX-16 differential refractometer. The molecular weight of hydrolyzed poly(maleic anhydride-*alt*-ethyl vinyl ether) was measured in 1 M NaCl solution.

Viscometry

Viscosity measurements were conducted with a Contraves LS-30 low shear rheometer at a constant shear rate of 1.3 s⁻¹ at 25 °C.

Polymer Synthesis and Characterization

One synthetic objective of this work was to prepare the amphipathic water-soluble polymers with controlled placement of fluorescence labels. The random incorporation of the labels was achieved by first synthesizing a functionalized naphthalene derivative shown in Scheme 1. The synthetic procedures for preparation of 1-(7-aminoheptyloxymethyl)naphthalene (**3**) proved to be

facile with satisfactory yields. The spacer length (in this case, heptyl) can be altered to decouple the naphthalene from the polymer backbone.

The model compound succinic acid, 7-(1-naphthylmethoxy) heptyl monoamide (**4**) (Scheme 2) was designed for fluorescence and UV studies. The sodium salt form is soluble in aqueous media.

Hydrophobically modified MA/EVE terpolymers (**7**) were prepared utilizing the synthetic procedures shown in Scheme 3. Terpolymers are designated by the number 7 followed by 8 or 12 designating octyl or dodecyl substitution. The final number represents the mole % incorporation. Initially, maleic anhydride/ethyl vinyl ether copolymer (**5**) was prepared in benzene. Characteristic of the free radical copolymerization is virtually complete alternation with little tendency of either monomer to homopolymerize.³ The M_w of the copolymer obtained by light scattering in this study was 2.4×10^5 g/mol.

Effects of Hydrophobic Groups

In order to assess the effects of hydrophobic monomer content on viscosity behavior in deionized water, it was first necessary to determine intrinsic viscosity utilizing the Fuoss relationship.⁴ Figure 1 shows the intrinsic viscosities of 7-C8 and 7-C12 terpolymers as a function of composition. The intrinsic viscosities decrease dramatically as the hydrophobe concentration in the terpolymers increases from 0 to 50 mole%, indicating intramolecular hydrophobic associations.⁵ A larger quantity of hydrophobic groups effectively enhances the hydrophobic interactions, resulting in collapse of the polymer coil. A sharp drop in the intrinsic viscosity was observed at hydrophobe concentrations between 20 and 30 mole% for both 7-C8 and 7-C12 terpolymers. Similar observations have been reported for other intramolecular associative copolymers⁵⁻⁸ and have been attributed to a transition from random coil to tighter hypercoil. Dodecyl terpolymers possess more compact structure than their octyl analogs at constant hydrophobe levels as indicated by the slightly lower intrinsic viscosities of the former (Figure 7).

Effect of pH

The amphipathic terpolymers contain a large number of carboxyl functionalities as the major hydrophilic component. Variation in pH can impart significant change in solution properties. Figure 2 illustrates the viscosity behavior of the terpolymers containing varying n-octyl concentration at selected pH values. The reduced viscosities of all the polymer solutions initially increase with increasing pH and then decrease. The maximum value of reduced viscosity for all 7-C8 polymers is observed about pH 9.5. Changes in the reduced viscosity are qualitatively similar to those observed for maleic anhydride and alkyl vinyl ether copolymers.⁹⁻¹¹ The degree of ionization of the terpolymers increases with increasing pH, disrupting intramolecular associations. The terpolymers reach maximum charge density at the pH at which the highest reduced viscosity is achieved. Further increase in pH increases the concentration of sodium ions in the solution; therefore, the interaction between the charged groups along the polymer backbone is shielded causing the polymer coil collapse.

When the pH of the solution is below the pK_a of the carboxylic acid, most, if not all, of the charges carried by the terpolymers are neutralized. Therefore, there are not enough charged groups

on the surface of polymer coil to prevent macromolecular aggregation and macrophase separation occurs. For example, the terpolymers with 40 and 50 mole% octyl groups precipitate below pH 4 and 5, respectively.

Effect of Electrolyte Addition

The effects of NaCl on the viscosity of the terpolymer solutions were investigated using 7-C8 series (Figure 3). The reduced viscosity decreases for all terpolymers as the NaCl molality increases due to the shielding of ionic interactions of the carboxylate groups. The terpolymers with high hydrophobe content such as 7-C8-50 precipitate at high salt concentration (ca. 0.5 M).

Photophysical Studies

Fluorescence measurements were conducted in an attempt to evaluate associative properties of the terpolymers in aqueous solutions. Naphthalene excimer to monomer ratios (I_E/I_M) were recorded to monitor the changes of terpolymer conformation. Terpolymers also show a dramatic hydrophobe concentration dependence of I_E/I_M . As indicated in Figure 4, I_E/I_M values of the terpolymers increase as the hydrophobe concentration varies from 10 to 30 mole%. Further increase in the hydrophobe concentration results in a decrease in I_E/I_M . It is unlikely that excimer formation is due to nearest neighbor interactions since the number of naphthyl groups is small and they are separated over a large distance along the polymer backbone. The initial increase in I_E/I_M may be attributed to the increased compaction of the polymer coil, which facilitates the formation of the excimer due to the reduced separation of the chromophore within the hydrophobic microdomain. When the hydrophobe concentration is above 30 mole%, the large hydrophobe quantities within the polymer coil separate the naphthyl labels. Furthermore, the highly compact hydrophobic microdomains limit the mobility of the chromophores, preventing orientation in a manner favorable for excimer formation. The latter effect has been observed previously by our group¹² and elsewhere¹³ for naphthalene-labelled methacrylic acid copolymers. The negligible formation of excimer in 7-C8-50 and 7-C12-40 which have high hydrophobe concentrations lends credence to these arguments.

TASK 3 - Solution Properties

Factorial Experimental Design For Characterizing Polymer Solutions by Light Scattering

Background

When analyzing information on polymer solutions from both static light scattering (SLS) and dynamic or quasielastic light scattering (DLS) experimentation, linear regression is used to fit data to theoretical relationships. These relationships are polynomial equations and contain two independent variables, sample concentration and scattering angle, and a response or dependent variable which is related to radiation intensities, as is the case for SLS, or apparent translational diffusion coefficients for DLS. The coefficients of the polynomials can be related to macromolecular parameters such as molecular weight, coil radius of gyration, hydrodynamic coil size, and solvent-polymer interaction.

A major difficulty in data analysis involves determining which polynomial model is appropriate when dealing with real data that contains random experimental noise. The noise level can be especially high for aqueous polymer solutions that tend to attract and retain dust. Thus, the experimenter is forced to deal with the high uncertainty always introduced into the scattering data by a large level of noise and a statistical approach must be used to analyze the data.

Light Scattering Test Model

In the case of light scattering, a good model for the experiment is a polynomial equation of the form

$$R = B_0 + B_1 X + B_2 X^2 + B_3 XY + B_4 Y + B_5 Y^2 \quad (1)$$

In Equation 1, R is the measured response and is dependent upon the independent variables X and Y which are set by the experimenter. The B parameters are the coefficients which are to be estimated by fitting Equation 1 to the experimental data obtained from a set of test conditions. In light scattering, X is the square of the sin of half the scattering angle, θ , and Y is the polymer concentration, C, in the solution scattering the radiation.

$$X = \sin^2(\theta/2) \quad (2) \quad Y = C \quad (3)$$

The response variable, R, measured at each test condition, depends upon the type of scattering experiment. For SLS

$$R = \frac{KC}{R_0} \quad (4)$$

where K is an optical constant and R_0 is the Rayleigh ratio which is a measure of the intensity of the scattered radiation at angle θ . For DLS, R is the apparent translational diffusion coefficient, D_{app} , measured at the test condition.

$$R = D_{app} \quad (5)$$

The test model proposed for light scattering is consistent with theoretical expectations for linear macromolecules that behave as random coils in solution. However, some terms in the test model may not be justified depending upon the polymer-solvent system under study and the noise level. After regression, all B coefficients not justified in the test model will be set to zero. In most cases, a simpler model, having fewer terms, will evolve after fitting the test model to the light scattering data.

Orthogonal Factorial Test Design

When using light scattering to characterize a polymer, it is convenient to measure responses using four sample concentrations. At each sample concentration four scattering angles are used. Thus 16 test conditions are established when characterizing a polymer solution by light scattering.

The scattering can usually be conducted such that both sample concentrations and angles of measurement are equally spaced so that a factorial experimental design can be performed¹⁶. Independent variables can then be scaled or transformed into a coded space. For example, if X and Y are varied by spacings $2\Delta X$ and $2\Delta Y$, respectively, such that four levels exist for each variable, then the coded space variables, x and y, can be defined by Equations 6 and 7. Each coded independent variable will have four values, -3, -1, 1, and 3, which represent the four test condition levels, low, middle low, middle high, and high, respectively.

$$x = \frac{X - \bar{X}}{\Delta X} \quad (6) \quad y = \frac{Y - \bar{Y}}{\Delta Y} \quad (7)$$

In the equations above \bar{X} and \bar{Y} are the averages of the four X and four Y values, respectively.

We can now write the following coded space test model for each of the 16 test conditions.

$$R_i = b_0 + b_1 x_i + b_2 x_i^2 + b_3 x_i y_i + b_4 y_i + b_5 y_i^2 \quad (8)$$

We can center Equation 8 by subtracting the average of all test condition responses, $\bar{R} = b_0 + 5b_2 + 5b_5$. This operation gives

$$R_i - \bar{R} = b_1 x_i + b_2 (x_i^2 - 5) + b_3 x_i y_i + b_4 y_i + b_5 (y_i^2 - 5) \quad (9)$$

We can use Equation 9 to write 16 equations that describe the test conditions. These equations can then be arranged into a 4^2 factorial design (two independent variables each having four levels) to form a set of orthogonal polynomial equations. Table I shows how the test conditions should be arranged to obtain a set of equations having orthogonal properties. Linear regression can then be performed on this set of equations to estimate the values of the coded coefficients in the scaled and centered test model, Equation 9.

Linear Regression in Coded Space

Matrix algebra can be used on the set of orthogonal equations formed by Equation 9 to find the vector \underline{b} which has the estimated values of coded space coefficients b_1 through b_5 . Coefficient b_0 can be found by noting that $b_0 = \bar{R} - 5(b_2 + b_5)$. The matrix operation to find the vector \underline{b} is given by

$$\underline{b} = (\underline{M}^T \underline{M})^{-1} \underline{M}^T (\underline{R} - \bar{R}) \quad (10)$$

where \underline{R} is the response vector, and \underline{M} is the matrix of coded test conditions given in Table II.

Confidence Interval for Coded Space Test Model Coefficients

The variance of the six coefficients in the vector \underline{b} can be determined if the experimental standard error associated with the test conditions, s_e , can be estimated. Replications of test conditions can be used to estimate s_e . If g test conditions are truly replicated, then the variance of each set of z measurements at each test condition, v , having $z - 1$ degrees of freedom, can be pooled to find an estimate of s_e by the following relationship¹⁷.

$$s_e^2 = \frac{\sum_{i=1}^s (v_i)(z_i - 1)}{\sum_{i=1}^s (z_i - 1)} \quad (11)$$

The elements on the diagonal of the variance-covariance matrix, \underline{V} , contain the variances for the coefficients b_1 to b_5 of vector \underline{b} . This matrix can be evaluated by the following operation

$$\underline{V} = (\underline{M}^T \underline{M})^{-1} s_e^2 \quad (12)$$

Because of the orthogonal experimental design, the covariance terms (elements not on the diagonal) in the matrix \underline{V} will be zero. No variance exists due to interactions between coefficients. Thus the estimated standard error of each coefficient, s_1 through s_5 , is the square root of its variance found in matrix \underline{V} . However, because b_0 is calculated from the values of b_2 and b_5 , its variance, s_0 , must be calculated from the square root of variance v_0 given by

$$v_0 = 25v_2 + 25v_5 + V_{0,0} \quad (13)$$

A Student "t" distribution can now be used to make confidence limits on each coefficient. The $(1-\alpha)$ confidence limits for each of the six coefficients are given by $(b_j \pm t_{\alpha/2} s_j)$. A good value to use for the significance, α , is 0.10 (90% confidence). The tabulated value for $t_{0.05}$ at 10 degrees of freedom is 1.81.

If the confidence limit for a b coefficient overlaps with zero, that coefficient cannot be justified and its value can be set to zero. Thus this "t" test eliminates unjustified terms in the coded test model and prevents overfitting of the data to a model having too many parameters. If b_2 or b_5 is eliminated (set to zero) by the "t" test, then the values for b_0 and s_0 should be recalculated.

Coefficients of the Real Space Test Model

After the values of the coefficients in the coded test model have been determined, then the coefficients for the real space test model can be calculated from the following relationships.

$$B_0 = b_0 - \frac{b_1 \bar{X}}{\Delta X} + \frac{b_2 \bar{X}^2}{\Delta X^2} + \frac{b_3 \bar{XY}}{\Delta X \Delta Y} - \frac{b_4 \bar{Y}}{\Delta Y} + \frac{b_5 \bar{Y}^2}{\Delta Y^2} \quad (14)$$

$$B_1 = \frac{b_1}{\Delta X} - \frac{2b_2 \bar{X}}{\Delta X^2} - \frac{b_3 \bar{Y}}{\Delta X \Delta Y} \quad (15) \quad B_2 = \frac{b_2}{\Delta X^2} \quad (16)$$

$$B_3 = \frac{b_3}{\Delta X \Delta Y} \quad (17) \quad B_4 = \frac{b_4}{\Delta Y} - \frac{2b_5 \bar{Y}}{\Delta Y^2} - \frac{b_3 \bar{X}}{\Delta X \Delta Y} \quad (18)$$

$$B_5 = \frac{b_5}{\Delta Y^2} \quad (19)$$

After substitution of the values for coefficients B_0 through B_5 , Equation 1 can be evaluated using a surface analysis technique originally developed by Zimm ¹⁵.

Surface Analysis of the Model Equation

Using Zimm's technique, experimental measurements of scattering response, KC/R_e for SLS or D_{app} for DLS, are plotted as the ordinate verses a compound abscissa, $\sin^2(\theta/2) + kC$. Use of the compound abscissa forces the points on the plot to be displaced from each other. This effect is due to the spacing constant k which is arbitrarily selected to provide adequate distance between the experimental data points.

The model equation developed from the 4^2 factorial design and justified by the "t" test can be used to plot the four constant concentration curves, the four constant angle curves, the zero concentration curve and the zero angle curve associated with the experimental data in the Zimm plot. Both curves will intercept the ordinate at the same position and this intersection point will be equal to the model equation coefficient B_0 .

The intersections of the constant concentration curves with the constant angle curves are the model equation fit points that correspond to the 16 data points on the plot. Thus, a visual understanding of the model equation fit to the experimental data can be realized by noting the placement of data points relative to curve intersections.

Use of the above factorial design experimentation and plotting procedures can best be demonstrated by giving two examples. In Example 1, a static light experiment was performed on a water soluble copolymer. In Example 2, the same copolymer was characterized by dynamic light scattering.

Experimental

The high molecular weight random copolymer employed in the scattering experiments was supplied by C. L. McCormick and was synthesized from acrylamide (AM) and 3-acrylamido-3-methylbutanoic acid (AMBA) monomers in the ratio of 95 to 5 as described in previous publications^{18, 19}. The aqueous solvent used to make the polymer solutions contained 0.514 M NaCl and had a refractive index, n , of 1.338 at 25 °C with radiation having a wavelength, λ_o , of 6328 Å.

Four solutions were made that had polymer concentrations of 0.04, 0.08, 0.12, and 0.16 g / liter. Light scattering experiments were performed on these solutions at 25 °C and at scattering angles of 32.3, 65, 90 and 115 degrees using a BI-2030AT goniometer equipped with a BI-DS photomultiplier and digital correlator manufactured by Brookhaven Instruments Corp. of Holtsville, NY. Duplicate measurements of intensity response, as KC/R_θ , were made for each of the 16 test conditions in SLS. Triplicate measurements of the apparent translational diffusion coefficient, D_{app} , were made for each of the 16 test conditions in DLS. The optical constant, K, used in SLS was calculated using a dn/dc value of 0.1559 ml / g for the polymer-solvent system under study. The change in the refractive index with respect to solution concentration, dn/dc , was measured using a KMX-16 differential refractometer manufactured by Chromatix Inc. of Sunnyvale, CA. The Zimm plots were generated using a spacing constant, k, of 5000 ml / g.

EXAMPLE 1 (STATIC LIGHT SCATTERING)

The theoretical relationship between the properties of a polymer sample in solution and its light scattering characteristics is expressed by the Debye relationship²⁰ given by Equation 20.

$$\frac{KC}{R_\theta} = \frac{1}{M_w} + \frac{16\pi^2 n^2 R_g^2 \sin^2(\frac{\theta}{2})}{3M_w \lambda_o^2} - \frac{64\pi^4 n^4 R_g^4 \sin^4(\frac{\theta}{2})}{3M_w \lambda_o^4} + 2A_2 C + 3A_3 C^2 + \text{other terms} \quad (20)$$

In Equation 20, M_w and R_g are the polymer weight average molecular weight and the "z" average polymer coil radius of gyration, respectively. The second and third viral coefficients, A_2 and A_3 are related to solvent-polymer interactions. Note that Equation 20 can be expressed as test model Equation 1 when we let the variables

$$R = \frac{KC}{R_g} \quad (21) \quad X = \sin^2\left(\frac{\theta}{2}\right) \quad (22) \quad Y = C \quad (23)$$

and let the B coefficients be defined as

$$B_0 = \frac{1}{M_w} \quad (24) \quad B_1 = \frac{16 \pi^2 n^2 R_g^2}{3 M_w \lambda_o^2} \quad (25) \quad B_2 = -\frac{64 \pi^4 n^4 R_g^4}{3 M_w \lambda_o^4} \quad (26)$$

$$B_3 = \text{interaction coefficient} \quad (27) \quad B_4 = 2A_2 \quad (28) \quad B_5 = 3A_3 \quad (29)$$

Note that we have defined the "other terms" in Equation 20 as a single expression equal to the product of an interaction coefficient, B_3 , and variables X and Y.

Values for X are 0.077, 0.289, 0.500, and 0.711. Thus, $2\Delta X = 0.211$ and $\bar{X} = 0.394$. Recall values for Y are 0.04, 0.08, 0.12, and 0.16 g / liter. Thus, $2\Delta Y = 0.04$ g / liter and $\bar{Y} = 0.10$ g / liter. Because of the equal separation of the values used for independent variables X and Y, we can use a 4^2 factorial design and then do a regression analysis to find estimates of the model coefficients. Thereafter we can use a "t" test to justify each coefficient of the model.

Scattering experiments were performed according to the design shown by Table I. The responses, KC/R_g in moles per gram, to the test conditions are shown in Table III. Two measurements were taken at each condition. The average at each test condition of the two measurements was used to form the response vector, \mathbf{R} , and is shown in the last column of Table III. Because two response measurements were taken at each test condition, Equation 11 could be used to estimate the average experimental error, s_e , associated with a response to a test condition. The s_e value obtained was 5.15×10^{-8} mole per gram. The average of all responses, \bar{R} , was 6.92×10^{-7} mole per gram.

The coded and scaled test model, Equation 9, can now be solved for the b coefficients using Equation 10. The results, vector \mathbf{b} , are shown in Table IV along with the upper and lower 90% confidence limits. The limits were calculated by solving for the matrix \mathbf{Y} and then

calculating the limits ($b_j \pm t_{0.05} s_j$) after finding the s_j values from the square root of the χ diagonal elements.

Inspection of Table IV shows that coefficients b_3 and b_5 are not significantly different from zero and thus their values and variances will be set to zero in subsequent calculations. Because b_5 was set to zero, b_0 was recalculated as 7.21×10^{-7} . Equations 14 through 19 can now be used to find the test model B coefficients. Next Equations 24, 25 and 27 can be used to find the polymer parameters M_w , R_g and A_2 . The B coefficients and the polymer parameters are listed in Table V.

Figure 3, a Zimm plot, shows the average response for each test condition as "X" symbols which are superimposed onto the curves constructed from the test model. Curves of constant angle are shown solid, curves of constant concentration are shown dashed, and the extrapolated zero concentration and zero angle curves are both shown dotted. The plot shows that the fit of the model equation to the experimental data is good.

EXAMPLE 2 (DYNAMIC LIGHT SCATTERING)

The apparent translational diffusional coefficient, D_{app} , obtained by DLS is related to the true diffusional coefficient, D_{true} , by the relationship

$$D_{app} = D_{true} + \alpha \sin^2\left(\frac{\theta}{2}\right) + \beta \sin^4\left(\frac{\theta}{2}\right) + \chi C \sin^2(\theta/2) + \delta C + \xi C^2 \quad (30)$$

The coefficients, D_{true} , α , β , χ , δ , ξ , are related to polymer-solvent properties. The parameters δ and ξ are usually referred to as the second and third diffusional viral coefficients. They are related to the interactions between solvent and polymer. The parameter D_{true} is the diffusional coefficient in the limit of zero polymer concentration and zero scattering angle and is related to the hydrodynamic polymer coil radius, R_h , by the Stokes-Einstein equation.

$$R_h = \frac{k_B T}{6 \pi \eta_0 D_{true}} \quad (31)$$

In Equation 31, k_B is the Boltzman constant, T is the absolute temperature, and η_0 is the solvent viscosity. For random coil polymers in solution, the coefficients α and β are expected to be related to D_{true} and R_g by the following relationships ²¹.

$$\alpha = \frac{16 \pi^2 n^2 D_{true} R_g^2}{5 \lambda_0^2} \quad (32) \quad \beta = \frac{-128 \pi^4 n^4 D_{true} R_g^4}{5 \lambda_0^4} \quad (33)$$

The coefficients δ and ξ are related to D_{true} and the polymer intrinsic viscosity, $[\eta]$.

$$\delta = \kappa D_{true} [\eta] \quad (34) \quad \xi = v D_{true} [\eta]^2 \quad (35)$$

The proportionality constants, κ and v , are expected to have values of 1.56 and -6.83, respectively²⁴. Jamieson¹⁴ has suggested that κ may have a lower value of 0.58.

Equation 30 can be expressed as test model Equation 1 when we let the variables be defined as

$$R = D_{app} \quad (36) \quad X = \sin^2\left(\frac{\theta}{2}\right) \quad (37) \quad Y = C \quad (38)$$

and let the B coefficients be defined as

$$B_0 = D_{true} \quad (39) \quad B_1 = \alpha \quad (40) \quad B_2 = \beta \quad (41)$$

$$B_3 = \chi \quad (42) \quad B_4 = \delta \quad (43) \quad B_5 = \xi \quad (44)$$

Values for X , $2\Delta X$, \bar{X} , Y , $2\Delta Y$, and \bar{Y} are the same as in Example 1. The DLS responses, D_{app} values in cm^2/sec , are shown in Table VI. Three measurements were taken at each test conditions. The average at each test condition was used to form the response vector, \mathbf{R} , and is shown in the last column of Table VI. As in the SLS example, an experimental error, s_e , was calculated to be $1.47 \times 10^{-9} \text{ cm}^2/\text{sec}$. The average response, \bar{R} , was $3.13 \times 10^{-8} \text{ cm}^2/\text{sec}$.

The coded and scaled test model, Equation 9, can now be solved for the b coefficients using Equation 10. The results, vector \mathbf{b} , are shown in Table VII along with the upper and lower 90% confidence limits calculated by solving for the matrix \mathbf{U} and then calculating the limits $b_j \pm t_{0.05} s_j$ after finding the s_j values from the \mathbf{U} diagonal elements.

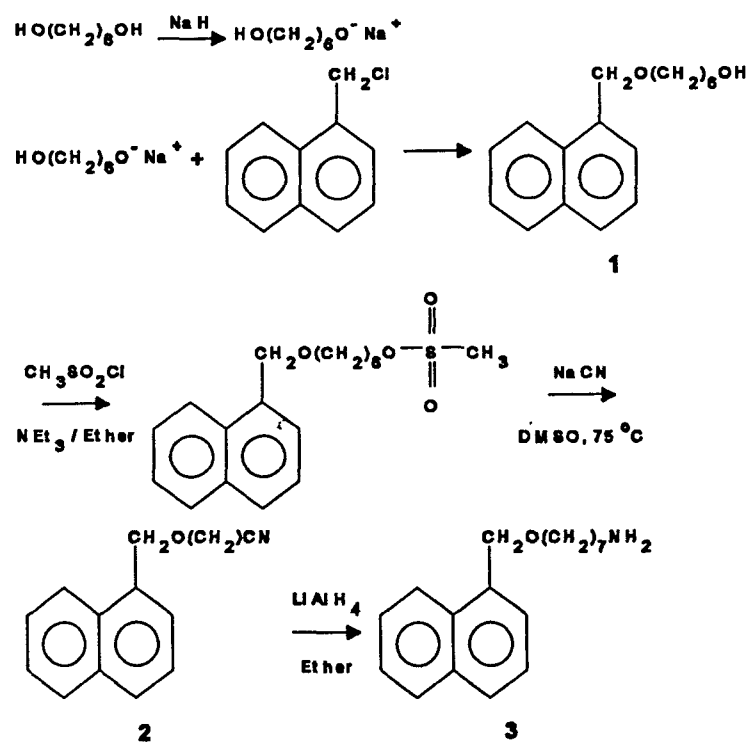
Inspection of Table VII shows that coefficients b_3 , b_4 and b_5 are not significantly different from zero and thus their values will be set to zero in subsequent calculations. Because b_5 was set to zero, b_0 and was recalculated as 3.39×10^{-8} . Equations 14 through 19 can now be used to find the test model B coefficients. Next Equations 36 and 31 can be used to find D_{true} and the

hydrodynamic polymer coil radius, R_h . The polymer coil radius of gyration, R_g , can be calculated from Equation 32. The B coefficients and polymer parameters are listed in Table VIII. Figure 4 is the Zimm plot for the DLS example. The fit of experimental data is shown to be adequate.

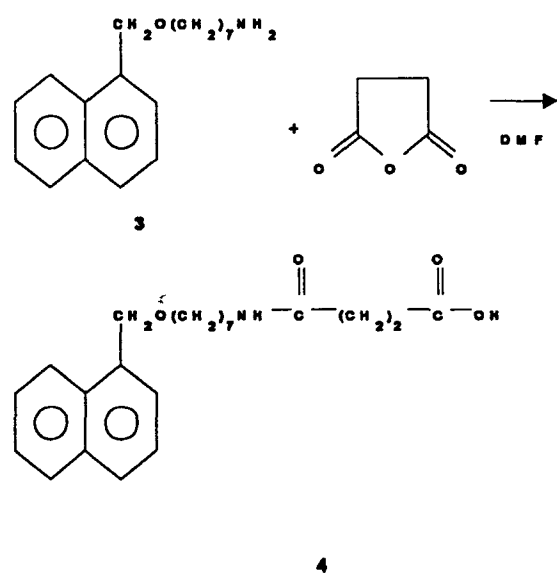
Conclusions

The data analysis technique detailed above which employs a factorial experimental design can be used to establish a light scattering model which is statistically justified. The model can thereafter be used to estimate macromolecular parameters such as polymer coil size, viral and diffusional coefficients, and molecular weight.

Scheme 1. Synthesis of 1-(7-Aminoheptyloxyethyl) naphthalene (**3**).



Scheme 2. Synthesis of naphthalene-containing model compound 4.



Scheme 3. Synthesis of hydrophobically modified maleic anhydride and ethyl vinyl ether-based terpolymers (7).

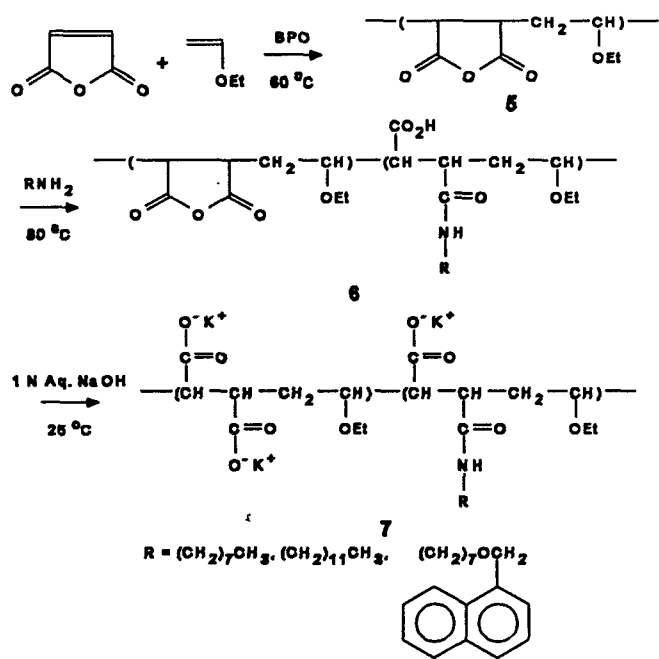


Figure 1. Effects of n-octyl and n-dodecyl group content on the intrinsic viscosity of 7-C8 and 7-C12 terpolymers in deionized water.

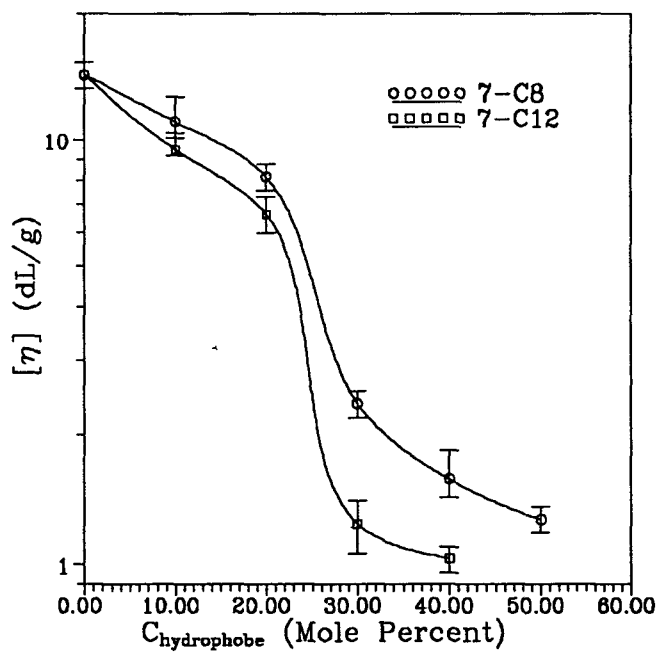
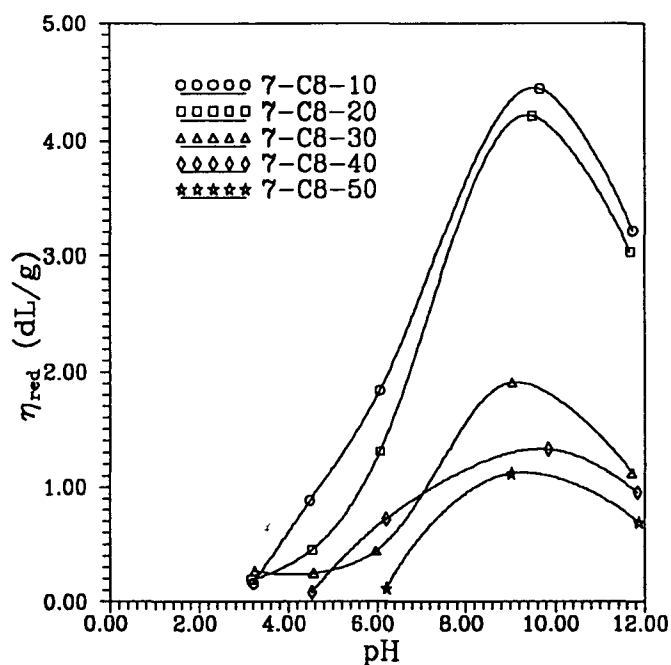


Figure 2. Effects of solution pH on η_{red} for 7-C8 polymers at 25 °C. $C_p = 0.5$ g/dL. Shear rate: 1.3 s⁻¹.



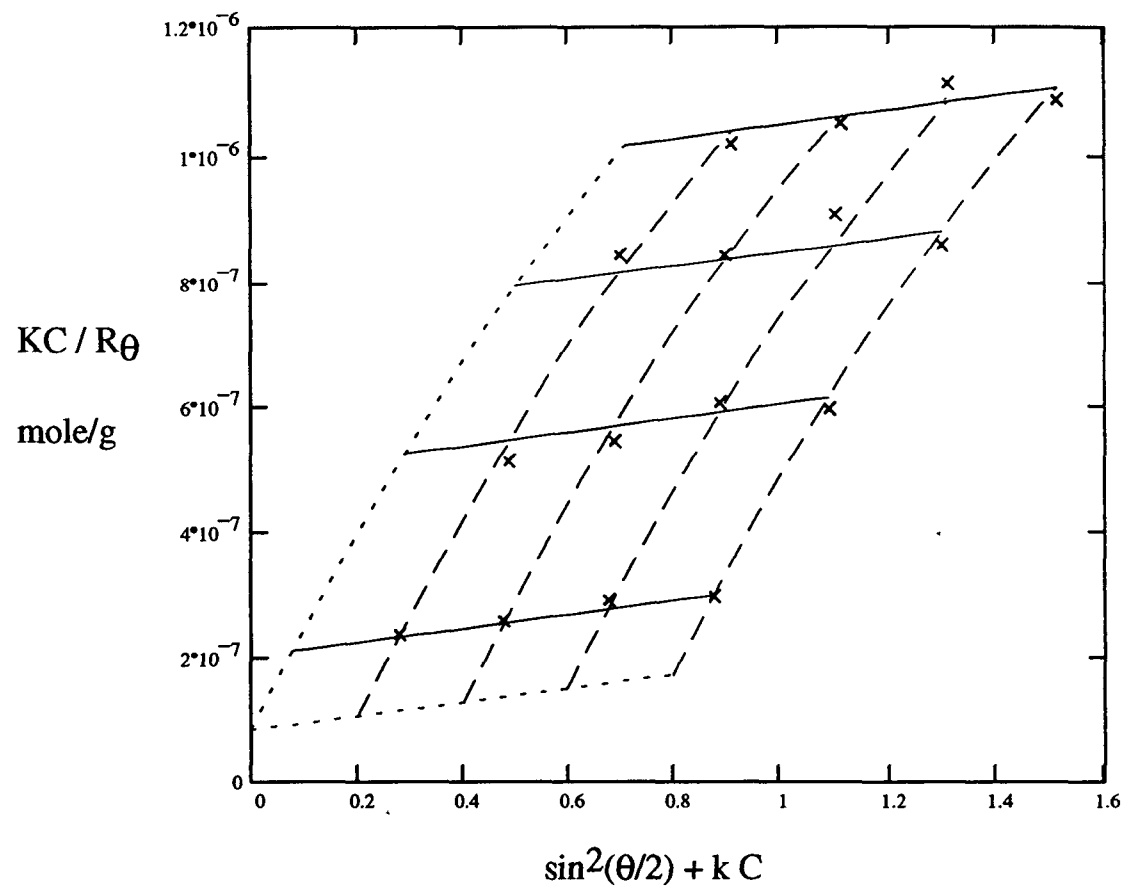


Figure 3 : Zimm Plot for Example 1 (SLS)

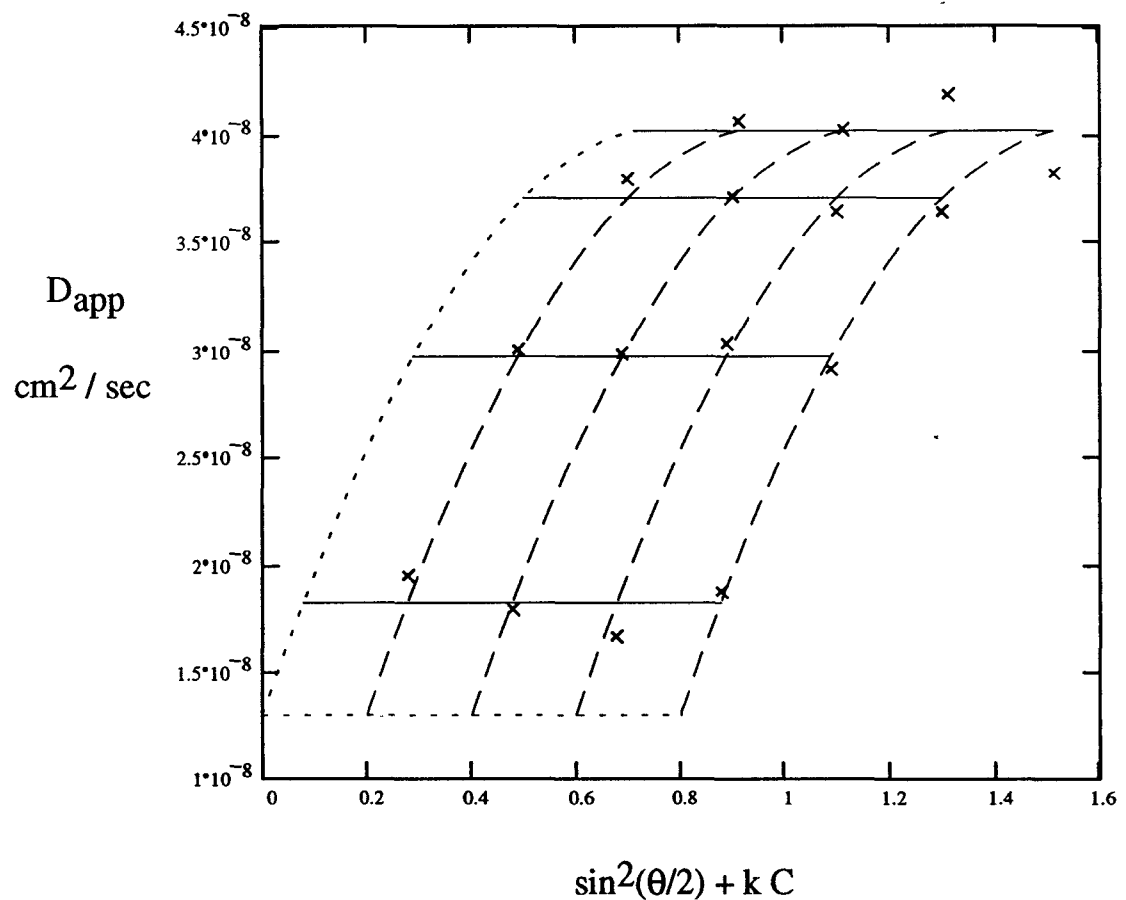


Figure 4 : Zimm plot for Example 2 (DLS)

TABLE I
4² EXPERIMENTAL FACTORIAL DESIGN

Test Condition Number	Coded Level For Independent Variable x	Coded Level For Independent Variable y
1	-3	-3
2	-3	-1
3	-3	1
4	-3	3
5	-1	-3
6	-1	-1
7	-1	1
8	-1	3
9	1	-3
10	1	-1
11	1	1
12	1	3
13	3	-3
14	3	-1
15	3	1
16	3	3

TABLE II
Matrix M

	x	$x^2 - 5$	xy	y	$y^2 - 5$
1	-3	4	9	-3	4
1	-3	4	3	-1	-4
1	-3	4	-3	1	-4
1	-3	4	9	3	4
1	-1	-4	3	-3	4
1	-1	-4	1	-1	-4
1	-1	-4	-1	1	-4
1	-1	-4	-3	3	4
1	1	-4	-3	-3	4
1	1	-4	-1	-1	-4
1	1	-4	1	1	-4
1	1	-4	3	3	4
1	3	4	-9	-3	4
1	3	4	-3	-1	-4
1	3	4	3	1	-4
1	3	4	9	3	4

Table III
Example 1 (SLS) Responses

Test Condition	Measurement 1 mole / g x 10 ⁷	Measurement 2 mole / g x 10 ⁷	Average Response mole / g x 10 ⁷
1	2.60	2.15	2.38
2	2.53	2.67	2.60
3	2.81	2.97	2.89
4	3.10	2.81	2.96
5	5.55	4.75	5.15
6	5.43	5.50	5.47
7	5.84	6.26	6.05
8	6.29	5.62	5.96
9	9.68	7.21	8.45
10	8.60	8.31	8.46
11	9.06	9.12	9.09
12	9.25	7.99	8.62
13	11.28	9.07	10.18
14	10.66	10.33	10.50
15	10.84	11.37	11.11
16	11.62	10.10	10.86

Table IV
Example 1 (SLS) Coded Test Model Coefficients

Coefficient	Estimated Value	Standard Error	Confidence Limits	
			Upper	Lower
b_0	$7.34 \times 10^{-7}*$	2.61×10^{-8}	7.81×10^{-7}	6.87×10^{-7}
b_1	1.34×10^{-7}	5.76×10^{-9}	1.45×10^{-7}	1.24×10^{-7}
b_2	-5.90×10^{-9}	3.22×10^{-9}	-7.45×10^{-11}	-1.17×10^{-8}
b_3	1.63×10^{-11}	2.57×10^{-9}	4.68×10^{-9}	-4.64×10^{-9}
b_4	1.11×10^{-8}	5.76×10^{-9}	2.15×10^{-8}	6.51×10^{-10}
b_5	-2.52×10^{-9}	3.22×10^{-9}	3.30×10^{-9}	-8.35×10^{-9}

$$* b_0 = \bar{R} - 5(b_2 + b_5)$$

Table V
Example 1 (SLS) Test Model Coefficients and Polymer Parameters

Coefficient	Estimated Value	Polymer Parameter	Estimated Value
B_0	8.3×10^{-8}	Molecular Weight, M_w	1.2×10^7 g / mole
B_1	1.7×10^{-6}	Radius of Gyration, R_g	2900 Å
B_2	-5.3×10^{-7}	---	---
B_3	0	---	---
B_4	5.5×10^{-4}	Second Virial Coefficient, A_2	2.7×10^{-4} ml-mole / g ²
B_5	0	---	---

Table VI
Example 2 (DLS) Responses

Test Condition	Measurement 1 cm ² / sec x 10 ⁸	Measurement 2 cm ² / sec x 10 ⁸	Measurement 3 cm ² / sec x 10 ⁸	Average Response cm ² / sec x 10 ⁸
1	1.95	2.05	1.85	1.95
2	1.81	1.75	1.81	1.79
3	1.36	1.79	1.84	1.67
4	1.88	1.91	1.83	1.87
5	3.04	3.02	2.96	3.00
6	3.01	3.00	2.97	2.98
7	3.09	3.02	2.97	3.03
8	2.85	3.00	2.88	2.91
9	3.80	3.80	3.77	3.79
10	3.74	3.65	3.72	3.71
11	3.62	3.68	3.60	3.63
12	3.65	3.64	3.62	3.63
13	3.92	4.10	4.18	4.07
14	3.61	4.18	4.28	4.03
15	4.14	4.24	4.17	4.18
16	4.11	3.23	4.13	3.82

Table VII
Example 2 (DLS) Coded Test Model

Coefficient	Value	Standard Error	Confidence Limits	
			Upper	Lower
b_0	$3.38 \times 10^{-8}*$	7.44×10^{-10}	3.52×10^{-8}	3.25×10^{-8}
b_1	3.66×10^{-9}	1.64×10^{-10}	3.96×10^{-9}	3.37×10^{-9}
b_2	-5.18×10^{-10}	9.16×10^{-11}	-3.52×10^{-10}	-6.83×10^{-10}
b_3	-2.49×10^{-11}	7.33×10^{-11}	1.08×10^{-10}	-1.58×10^{-10}
b_4	-2.15×10^{-10}	1.64×10^{-10}	8.18×10^{-11}	-5.11×10^{-10}
b_5	5.57×10^{-12}	9.16×10^{-11}	1.71×10^{-10}	-1.60×10^{-10}

$$* b_0 = \bar{R} - 5(b_2 + b_5)$$

Table VIII
Example 2 (DLS) Test Model Coefficients and Polymer Parameters

Coefficient	Estimated Value	Polymer Parameter	Estimated Value
B_0	1.3×10^{-8}	True Diffusional Coefficient, D_{true}	1.3×10^{-8} cm^2/sec
B_1	7.1×10^{-8}	Radius of Gyration, R_g	2000 \AA
B_2	-4.6×10^{-8}	HydrodynamicRadius , R_h	1800 \AA

REFERENCES

1. Neuman, M.S.; Otsuka, S. *J. Org. Chem.* **1958**, *23*, 797.
2. Chang, Y.; McCormick, C.L. *Macromolecules* **1994**, *27*, 2151.
3. Baldwin, M.G. *J. Polym. Sci.* **1965**, *A3*, 703.
4. Fuoss, R.M.; Cathers, G.I. *J. Polym. Sci.* **1949**, *4*, 96.
5. Strauss, U.P.; Gershfeld, N.L.; Cook, E.H. *J. Phys. Chem.* **1956**, *60*, 577.
6. Ghesquiere, D.; Chachaty, C.; Ban, B.; Loucheux, C. *Makromol. Chem.* **1976**, *177*, 1601.
7. Strauss, U.P.; Vesnaver, G. *J. Phys. Chem.* **1975**, *79*, 1558.
8. Strauss, U.P.; Vesnaver, G. *J. Phys. Chem.* **1975**, *79*, 2428.
9. Strauss, U.P.; Schlesinger, M.S. *J. Phys. Chem.* **1978**, *82*, 1627.
10. Dubin, P.; Strauss, U.P. *J. Phys. Chem.* **1967**, *71*, 2757.
11. Dubin, P.; Strauss, U.P. *J. Phys. Chem.* **1970**, *74*, 2842.
12. McCormick, C.L.; Hoyle, C.E.; Clark, M.D. *Macromolecules* **1990**, *23*, 3124.
13. Seo, T.; Take, S.; Akimoto, T.; Hamada, K.; Iijima, T. *Macromolecules* **1991**, *24*, 4801.

14. Patterson, P.M. and A. M. Jamieson, *Macromolecules*, 18, 266, 1985.
15. Zimm, B. H., *J. Chem. Phys.*, 16, 1099, 1948.
16. Hicks, C. R., *Fundamental Concepts in the Design of Experiments*, Holt, Rinehart and Winston, N.Y., 95, 1964.
17. Box, G. P., W. G. Hunter, J. S. Hunter, *Statistics for Experiments*, John Wiley & Sons, N.Y., 319, 1978.
18. McCormick, C. L. and K. P. Blackmon, *J. Poly. Sci., Poly. Chem.*, A24, 2635, 1986.
19. McCormick, C. L., K. P. Blackmon, and D. L. Elliott, *J. Poly. Sci., Poly. Chem.*, A24, 2619, 1986.
20. Tanford, C., *Physical Chemistry of Macromolecules*, John Wiley & Sons, N.Y., 275, 1961.
21. Peitzsch, R. M., M. J. Burt, and W. F. Reed, *Macromolecules*, 25, 806, 1992.
22. Schmitz, K.S., *An Introduction to Light Scattering by Macromolecules*, Academic Press, Inc., N.Y., 181, 1990.